Physics Letters B 790 (2019) 64–70

Contents lists available at ScienceDirect

Physics Letters B

www.elsevier.com/locate/physletb

Probing relic neutrino radiative decays with 21 cm cosmology

M. Chianese [a], P. Di Bari [a,*], K. Farrag [a,b], R. Samanta [a]

[a] Physics and Astronomy, University of Southampton, Southampton, SO17 1BJ, UK
[b] School of Physics and Astronomy, Queen Mary, University of London, London, E1 4NS, UK

ARTICLE INFO

Article history:
Received 11 June 2018
Received in revised form 18 September 2018
Accepted 19 September 2018
Available online 21 September 2018
Editor: H. Peiris

ABSTRACT

We show how 21 cm cosmology can test relic neutrino radiative decays into sterile neutrinos. Using recent EDGES results, we derive constraints on the lifetime of the decaying neutrinos. If the EDGES anomaly will be confirmed, then there are two solutions, one for much longer and one for much shorter lifetimes than the age of the universe, showing how relic neutrino radiative decays can explain the anomaly in a simple way. We also show how to combine EDGES results with those from radio background observations, showing that potentially the ARCADE 2 excess can be also reproduced together with the EDGES anomaly within the proposed non-standard cosmological scenario. Our calculation of the specific intensity at the redshifts probed by EDGES can be also applied to the case of decaying dark matter.

1. Introduction

With 21 cm cosmology we are entering a new exciting phase in the study of the history of the universe and how this can be used to probe fundamental physics [1,2]. Observations of the redshifted 21 cm line of neutral hydrogen[1] from the emission or absorption of the cosmic microwave background radiation (CMB) by the intergalactic medium, can test the cosmic history at redshifts $z \sim 5$–1100.[2] This range corresponds to those three periods, after recombination, on which we have fragmentary information: the *dark ages*, from recombination at $z_{\rm rec} \simeq 1100$ to $z \simeq 30$, when first astrophysical sources start to form; the *cosmic dawn*, from $z \simeq 30$ to the time when reionisation begins at $z \simeq 15$; the *Epoch of Reionisation* (EoR), from $z \simeq 15$ to $z \simeq 6.5$ when reionisation ends.[3] In this way observations of the cosmological 21 cm line global signal can test the standard ΛCDM cosmological model during a poorly period of the cosmic history, considering that the most distant galaxy is located at $z = 11.1$ [4].

Intriguingly, the EDGES (*Experiment to Detect the Global Epoch of Reionisation Signature*) collaboration claims to have discovered an absorption signal in the CMB radiation spectrum corresponding to the redshifted 21 cm line at $z \simeq 17.2$ with an amplitude about twice the expected value [5]. This represents a $\sim 3.8\sigma$ deviation from the predictions of the ΛCDM model and for this reason the EDGES anomaly has drawn great attention. It should be said that another group [6], re-analysing publicly available EDGES data and using exactly their procedures, finds almost identical results but they claim that 'the fits imply either non-physical properties for the ionosphere or unexpected structure in the spectrum of foreground emission (or both)' concluding that their results 'call into question the interpretation of these data as an unambiguous detection of the cosmological 21-cm absorption signature.' Therefore, more observations will be necessary to confirm not only the anomaly but even the absorption signal.

In the light of these recent experimental developments, it is anyway interesting to think of possible non-standard cosmological scenarios that can be tested with 21 cm signal observations at high redshifts and that might either explain the EDGES anomaly (if confirmed) or in any case be constrained. The EDGES anomaly can be expressed in terms of a value of the photon-to-spin temperature ratio $T_\gamma(z)/T_S(z)$ at redshifts $z = 15$–20, where the absorption profile is observed, that is about twice what is expected in a standard cosmological scenario. This can be of course due either to a larger value of $T_\gamma(z)$ or a smaller value of $T_S(z)$ or some combination of the two. In this Letter, we show how radiative decays of the lightest relic neutrinos can explain the EDGES anomaly producing, after recombination, a non-thermal early photon background able

* Corresponding author.
E-mail addresses: M.Chianese@soton.ac.uk (M. Chianese), P.Di-Bari@soton.ac.uk (P. Di Bari), K.R.H.A.M.Farrag@soton.ac.uk (K. Farrag), romesamanta@gmail.com (R. Samanta).

[1] We refer to hydrogen-1 (protium). Deuterium has an analogous line but at 92 cm.

[2] We will discuss this range in more detail in Section 2.

[3] The redshift boundaries of these stages are, in fact, very model dependent. Definite values strongly depend on astrophysical parameters (e.g., see [3] for a recent parameter study). The approximate value $z \simeq 6.5$ for the end of EoR corresponds to a particular model shown in Fig. 1 in [1] and references therein.

https://doi.org/10.1016/j.physletb.2018.09.040

to rise $T_\gamma(z)$ above the CMB value. A similar scenario, recently revisited in [8], where heavier relic neutrinos decay radiatively into lighter ordinary neutrinos [9–11] is ruled out since it requires degenerate neutrino masses now excluded by the *Planck* upper bound $\sum_i m_i \lesssim 0.17\,\text{eV}$ (95% C.L.) [12] and since, it requires a too large effective magnetic moment responsible for the decay. In our scenario the lightest relic neutrinos decay radiatively into sterile neutrinos and this allows to circumvent both bounds.[4]

The paper is organised as follows. In Section 2 we briefly review 21 cm cosmology and the EDGES results. In Section 3 we discuss how lightest relic neutrinos radiative decays can explain the EDGES anomaly. Finally, in Section 4, we draw the conclusions.

2. 21 cm cosmology and EDGES results

The 21 cm line is associated with the hyperfine energy splitting between the two energy levels of the 1s ground state of the hydrogen atom characterised by a different relative orientation of electron and proton spins: anti-parallel for the singlet level with lower energy, parallel for the triplet level with higher energy. The energy gap between the two levels and, therefore, of the absorbed or emitted photons at rest, is $E_{21} = 5.87\,\mu\text{eV}$ corresponding to a 21 cm line rest frequency $\nu_{21}^{\text{rest}} = 1420\,\text{MHz}$.

A shell of neutral hydrogen at a given redshift $z \lesssim z_{\text{rec}}$, after recombination, can then act, thanks to the 21 cm transitions, as a detector of the background photons produced at higher redshifts. In standard cosmology this background is just given by the CMB thermal radiation with temperature $T_{CMB}(z) = T_{CMB,0}\,(1+z)$, where $T_{CMB,0} = 2.725\,\text{K} \simeq 2.35 \times 10^{-4}\,\text{eV}$.

This possibility relies on the *brightness contrast* between the intensity of the 21 cm signal from the shell of neutral hydrogen gas at redshift z and the background radiation at the observed (redshifted) frequency $\nu_{21}(z) = \nu_{21}^{\text{rest}}/(1+z)$. The brightness contrast can be expressed in terms of the *21 cm brightness temperature* (relative to the photon background) [14]:

$$T_{21}(z) \simeq 23\,\text{mK}\,(1+\delta_B)\,x_{H_I}(z)\left(\frac{\Omega_B h^2}{0.02}\right) \times \left[\left(\frac{0.15}{\Omega_{\text{m}} h^2}\right)\left(\frac{1+z}{10}\right)\right]^{1/2}\left[1 - \frac{T_\gamma(z)}{T_S(z)}\right], \tag{1}$$

where $\Omega_B h^2 = 0.02226$ and $\Omega_{\text{m}} h^2 = 0.1415$ [15] are respectively the baryon and matter abundances, δ_B is the baryon overdensity, x_{H_I} is the fraction of neutral hydrogen, $T_\gamma(z)$ is the effective temperature, at frequency $\nu_{21}(z)$, of the photon background radiation (coinciding with $T_{CMB}(z)$ in standard cosmology) and $T_S(z)$ is the *spin temperature* parameterising the ratio of the population of the excited state n_1 to that one of the ground state n_0 in such a way that

$$\frac{n_1}{n_0}(z) \equiv \frac{g_1}{g_0} e^{-\frac{E_{21}}{T_S(z)}}\,, \tag{2}$$

where $g_1/g_0 = 3$ is the ratio of the statistical degeneracy factors of the two levels. Clearly if x_{H_I} vanishes, then there is no signal, since in that case all hydrogen would be reionised and there cannot be any 21 cm transition. The spin temperature is related to T_{gas}, the kinetic temperature of the gas, by[5]

$$\left(1 - \frac{T_\gamma}{T_S}\right) \simeq \frac{x_c + x_\alpha}{1 + x_c + x_\alpha}\left(1 - \frac{T_\gamma}{T_{\text{gas}}}\right), \tag{3}$$

where x_α and x_c are coefficients describing the coupling between the hyperfine levels and the gas. In the limit of strong coupling, for $x_\alpha + x_c \gg 1$, one has $T_S = T_{\text{gas}}$, while in the limit of no coupling, for $x_\alpha = x_c = 0$, one has $T_S = T_\gamma$ and in this case there is no signal. The evolution of T_{21} with redshift can be schematically described by five main stages [1,2]:

(i) In a first stage after recombination, during the dark ages, the gas is still coupled to radiation thanks to a small but non negligible amount of free electrons that still interacts via Thomson scatterings with the photon background. In this case one has $T_\gamma = T_{\text{gas}} = T_S$ and consequently $T_{21} = 0$, i.e., there is no signal.[6] This stage lasts until the gas starts decoupling from radiation above $z_{\text{dec}}^{\text{gas}} \simeq 150$. At this time the gas temperature cools down more rapidly than CMB radiation, with $T_{\text{gas}}(z) = T(z_{\text{dec}})\,(1+z_{\text{dec}})^2$.

(ii) In a second stage, approximately for $250 \gtrsim z \gtrsim 30$, still during the dark ages and with the precise boundary values depending on different cosmological details, one has approximately $T_S \simeq T_{\text{gas}}$, since gas collisions are efficient enough to couple T_S to T_{gas}. In this case one has $T_{21} < 0$ and an early absorption signal is expected.

(iii) At $z \simeq 30$ the gas becomes so rarified that the collision rate becomes too low to enforce $T_S \simeq T_{\text{gas}}$ and in this case one enters a regime where $x_a + x_c \ll 1$ and $T_S \simeq T_\gamma$. In this stage, during the cosmic dawn, one has $T_{21} \simeq 0$ and again the 21 cm global signal is suppressed.[7]

(iv) At $z \simeq 30$, gas also starts collapsing under the action of dark matter and first astrophysical sources start to form with emission of Lyα radiation that is able, through Wouthuysen–Field effect [17], to gradually couple again T_S to T_{gas}. In the redshift range $z_h \lesssim z \lesssim 25$, where $z_h \simeq 10$–20 is the redshift at the heating transition [1] (this stage starts during the cosmic dawn and can last until the epoch of reionization has begun at $z \simeq 15$), one can again have $T_{21} < 0$, implying an absorption signal. This is within the range tested by EDGES whose results seem to confirm the existence of the absorption signal.

(v) In a fifth stage, for $z \lesssim z_h$ (depending on the precise value of z_h this stage can either start during cosmic dawn and ending during the epoch of reionization or entirely occurring during the latter), the gas gets reheated by the astrophysical radiation and $T_S \simeq T_{\text{gas}} > T_\gamma$, so that T_{21} turns positive and one has an emission signal from the regions that are not fully ionised. Eventually all gas gets ionised until the fraction of neutral hydrogen vanishes and the signal switches off again.[8]

EDGES High and Low band antennas probe the frequency ranges 90–200 MHz and 50–100 MHz respectively overall measuring the 21 cm signal from between redshift 6 and 27, which corresponds to an age of the universe between 100 Myr and 1 Gyr and includes the epochs of reionization and cosmic dawn, when first astrophysical sources form and a second stage of absorption signal is

[4] See end of Section 3 for more details on this point while for an updated review on neutrino mass constraints see for example [13].

[5] This is an approximated relation valid for $T_{\text{gas}} \simeq T_c$, where T_c is the colour temperature parameterising the intensity of the UV radiation emitted by the astrophysical sources. Notice that out of the four different temperatures we introduced, only T_{CMB} and T_{gas} are genuine thermodynamic temperatures associated to a thermal distribution.

[6] This conclusion is approximate and a very small signal is present even at high redshifts mainly due to the fact that T_c deviates slightly from T_{gas}. This has been studied recently in detail in [16] and it was found $-T_{21} \simeq 2.5\,\text{mK}$ at $z \simeq 500$.

[7] A detailed description and in particular how suppressed the signal is in this stage depends on various astrophysical parameters [3].

[8] In this stage the signal crucially depends on astrophysics and it should be said that not in all scenarios T_{gas} becomes larger than T_γ and in this case the emission signal is missing [18].

predicted (the fourth and fifth stage in the description above). The EDGES collaboration found an absorption profile approximately in the range $z = 15$–20 with the minimum at $z_{\rm E} \simeq 17.2$, corresponding to $\nu_{21}(z_{\rm E}) \simeq 78\,{\rm MHz}$, with a 21 cm brightness temperature $T_{21}(z_{\rm E}) = -0.5^{+0.2}_{-0.5}\,{\rm K}$ at 99% C.L., including estimates of systematic uncertainties. From Eq. (1), since $(1+\delta_{\rm b})\,x_{H_I}(z_{\rm E}) \simeq 1$, this translates into $T_\gamma(z_{\rm E})/T_S(z_{\rm E}) = 15^{+15}_{-5.5}$. On the other hand, at the centre of the absorption profile detected by EDGES, one expects, assuming the ΛCDM model, $T_\gamma(z_{\rm E}) = T_{CMB}(z_{\rm E}) = T_{CMB,0}\,(1+z_{\rm E}) \simeq 50\,{\rm K}$ and $T_{\rm gas}(z_{\rm E}) \simeq T_{CMB}(z^{\rm gas}_{\rm dec})\,(1+z_{\rm E})^2/(1+z^{\rm gas}_{\rm dec})^2 \simeq 7\,{\rm K}$, where we indicated with $z^{\rm gas}_{\rm dec} \simeq 150$ and $T^{\rm gas}_{\rm dec} \simeq 410\,{\rm K}$ respectively the redshift and the temperature at the time when the gas decoupled from radiation. From Eq. (1) one then immediately finds $T_{21}(z_{\rm E}) \gtrsim -0.2\,{\rm K}$, where the minimum is saturated for $T_S(z_{\rm E}) = T_{\rm gas}(z_{\rm E})$ and corresponds to $T_\gamma(z_{\rm E})/T_{\rm gas}(z_{\rm E}) \simeq 7$. Therefore, the best fit value for $T_{21}(z_E)$ is about 2.5 lower than expected within the ΛCDM. Even at 99% C.L. it is still 50% lower.

If this anomalous result will be confirmed and astrophysical solutions ruled out, then, very interestingly, it can be regarded as the effect of some non-standard cosmological mechanism. For example, it has been proposed that a (non-standard) interaction of the baryonic gas with the much colder dark matter component would cool down $T_{\rm gas}$, and consequently T_S, below the predicted ΛCDM value [7]. Another possibility is that $T_{\rm gas}$ is lower because the gas decouples earlier so that $z^{\rm gas}_{\rm dec} > 150$. For example for $z^{\rm gas}_{\rm dec} \simeq 300$, one has $T_{\rm gas}(z_{\rm E}) \simeq 3.5\,{\rm K}$, i.e., halved compared to the value predicted within the ΛCDM, and this would reconcile the tension between ΛCDM prediction and the EDGES result. Models of early dark energy have been proposed to this extent, but these are strongly ruled out by observations of the CMB temperature power spectrum [19]. A third possibility is that some non-standard source could produce a non-thermal additional component of soft photons effectively increasing T_γ above T at frequencies around $\nu_{21}(z_{\rm E})$. For example, these could be produced by dark matter annihilations and/or decays [20,21] and also give a signal at other frequencies for example addressing the ARCADE 2 excess at higher ($\sim$GHz) frequencies [22] that, however, has not been confirmed by another group using ATCA data [23]. Conversion of dark photons into soft photons has also been proposed as a solution to the EDGES anomaly [24].

In the next section we present a mechanism for the production of a non-thermal soft photon component relying on relic neutrinos radiative decays into sterile neutrinos. Even if the EDGES anomaly will not be confirmed, we show that the EDGES results tighten the existing constraints [10,25] on the parameters of the scenario.

3. Relic neutrino radiative decays

The 21 cm CMB photons absorbed at z_E fall clearly in the Rayleigh–Jeans tail since $E_{21} \ll T(z_{\rm E})$. In this regime the specific intensity depends linearly on temperature, explicitly

$$I_{CMB}(E,z) \equiv \frac{d\mathcal{F}_E^{\gamma_{CMB}}}{dA\,dt\,dE\,d\Omega} = \frac{1}{4\pi}\frac{d\varepsilon_{CMB}}{dE} = \frac{E^3}{4\pi^3}\,[e^{E/T_{CMB}}-1]^{-1} \overset{E\ll T_{CMB}}{\longrightarrow} \frac{1}{4\pi^3}\,T_{CMB}(z)\,E^2\,. \tag{4}$$

Only photons with energy E_{21} at $z \simeq z_{\rm E}$ could be absorbed by the neutral hydrogen producing a 21 cm absorption global signal. The EDGES results can be explained by an additional non-thermal photon background with $I_{\rm nth}(E_{21}, z_{\rm E}) \simeq I_{CMB}(E_{21}, z_{\rm E})$. The effective photon temperature $T_\gamma(E, z_E)$ at an arbitrary energy E can be simply calculated as

$$T_\gamma(E,z_E) = E\,\ln^{-1}\left(1+\frac{E^3}{4\pi^3\,I_\gamma(E,z_E)}\right) \overset{E\ll T_\gamma}{\longrightarrow} \frac{4\pi^3}{E^2}\,I_\gamma(E,z_E)\,, \tag{5}$$

where we defined $I_\gamma(E,z_E) = I_{\rm nth}(E,z_E) + I_{CMB}(E,z_E)$. The EDGES anomaly can be explained imposing $T_\gamma(E_{21},z_E)/T_{CMB}(z_E) = 2.15^{+2.15}_{-0.8}$, or, equivalently,

$$R \equiv \frac{I_{\rm nth}(E_{21},z_E)}{I_{CMB}(E_{21},z_E)} = \frac{T_{\gamma_{\rm nth}}(E_{21},z_E)}{T_{CMB}(z_E)} = R_E \equiv 1.15^{+2.15}_{-0.8}\,, \tag{6}$$

where $T_{\gamma_{\rm nth}}$ is defined in terms of $I_{\rm nth}$ in the same way as T_γ is defined in terms of I_γ in Eq. (5). We consider the radiative decay of active neutrinos ν_i with mass m_i and lifetime τ_i into a sterile neutrino ν_s with mass m_s, i.e., $\nu_i \to \nu_s + \gamma$. For definiteness we will refer to the case of lightest neutrino decays corresponding to $i = 1$. We will comment at the end how our results simply change if one considers heavier neutrinos. If decays occur after matter–radiation decoupling, photons produced from the decays will not distort CMB thermal spectrum but will give rise to a non-thermal γ background [10] contributing to R. For a given m_1 one has two limits for m_s: a quasi-degenerate limit for $m_1 \simeq m_s$ and a limit $m_s \ll m_1$.[9]

For $m_s \ll m_1$ the bulk of neutrinos, with $E \sim T_{CMB}$, necessarily decay when they are relativistic. This is easy to understand. Let us introduce the scale factor $a = (1+z)^{-1}$ and its corresponding value $a_E \equiv (1+z_E)^{-1}$ at z_E. In the matter-dominated regime we can write $a(t) \simeq a_E\,(t/t_E)^{\frac{2}{3}}$, where $t_{\rm E} \simeq 222\,{\rm Myr}$ is the age of the universe at $z = z_E$ [26]. For neutrinos that decay at rest at time t one has to impose $m_1 = 2\,E_{21}\,a_E/a(t)$ in order to have photons with the correct energy at t_E. Imposing that decays occur after recombination, otherwise the non-thermal component would thermalise or produce unacceptable distortions to the CMB spectrum, and of course before the time when photons are absorbed by neutral hydrogen, corresponding to a condition $z_{\rm E} < z(t) < z_{\rm rec} \simeq 1100$, one finds $0.012\,{\rm meV} \lesssim m_1 \lesssim 0.71\,{\rm meV}$, showing that the ν_1's are too light to be treated non-relativistically for $m_s \ll m_1$.[10]

On the other hand the non-relativistic case can be realised in the quasi-degenerate limit for $m_1 \simeq m_s$ since one can then have $m_1 \gg T_\nu(z) \simeq (4/11)^{1/3}\,T(z)$ at the time when they decay. Indeed at $z = z_E$ one has $T_\nu(z_E) \simeq 3\,{\rm meV}$. Since the current upper bound on the sum of neutrino masses implies $m_1 \lesssim 50\,{\rm meV}$, one can well have $m_1 \simeq m_s \gg 3\,{\rm meV}$. This implies $50 \gtrsim m_1/{\rm meV} \gtrsim 10$,[11] a window that will be fully tested by close future cosmological observations [28]. Moreover in this (testable) non-relativistic and quasi-degenerate case not only it is easy to calculate R, as we will see, but also one obtains the most conservative constraints on τ_1 and $\Delta m_1 \equiv m_1 - m_s$ since, as we will

[9] The origin and properties of neutrino masses and mixing would be related to extensions of the SM (e.g., grand-unified theories). Simplest models usually require the existence of very heavy sterile neutrinos ($m_s \gg 100\,{\rm GeV}$) in the form of right-handed neutrinos. However, the existence of light sterile neutrinos cannot be excluded and many models have been proposed especially in connection with different neutrino mixing anomalies (for a review see for example [27]).

[10] This also shows that the two heavier neutrinos radiative decays would produce photons at too high frequencies, considering that $m_2 \geq m_{\rm sol} \simeq 9\,{\rm meV}$ and $m_3 \geq m_{\rm atm} \simeq 50\,{\rm meV}$, where the lower bounds are saturated in the normal hierarchical limit. One could consider radiative decays $\nu_{2,3} \to \nu_1 + \gamma$ and in the quasi-degenerate limit $m_1 \gtrsim 0.12\,{\rm eV}$ photons with the correct energy would be produced. However, the upper bound $m_1 \lesssim 0.07\,{\rm eV}$ placed by the *Planck* collaboration now rules out this possibility [12]. Moreover these processes need values of the effective magnetic moment ruled out by current experimental upper bound [11,8].

[11] The lower bound $m_1 \gtrsim 10\,{\rm meV}$ corresponds to $m_1 \gtrsim 3\,T_\nu(z_E)$ that is quite a conservative condition to enforce that the bulk of neutrinos are non-relativistic when they decay since remember that for a Maxwell–Boltzmann distribution $\sqrt{\langle v^2\rangle} = \sqrt{3\,T/m}$. In this way the bulk of neutrinos have a kinetic energy that is negligible compared to the rest energy.

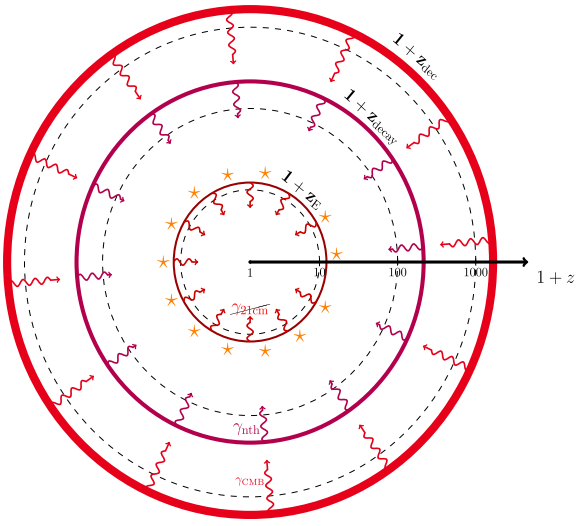

Fig. 1. Schematic picture describing the generation of the 21 cm absorption signal within a non-standard history of the universe including ν_1 radiative decays producing a non-thermal photon background. At redshifts $z \sim z_E$ the first astrophysical sources couple the spin temperature to the gas temperature (via Wouthuysen–Field effect) inducing the absorption of (redshifted) $\gamma_{21\,\rm cm}$ photons.

point out, if neutrinos decay relativistically, constraints get more stringent.

Let us then calculate R for $m_1 \simeq m_s \gg T_\nu(z)$. An emitted photon has an energy at decay $E = \Delta m_1$. Moreover let us suppose first that all neutrinos decay instantaneously at $t = \tau_1$ corresponding to a redshift $z_{\rm decay}$ such that $a_{\rm decay} = (1 + z_{\rm decay})^{-1} \simeq a_E\,(\tau_1/t_E)^{2/3}$. A sketchy representation of this toy model is given in Fig. 1. Requiring that photons produced from neutrino decays are then (21 cm) absorbed at $z = z_E$, one has to impose $\Delta m_1 = E_{21}\,a_E/a_{\rm decay}$, implying an unrealistic fine-tuned relation between τ_1, E_{21} and Δm_1. In addition it is easy to see that, since all photons produced in the decay contribute to the signal, one obtains a far too high value of R. This is because in this instantaneous decay description one has simply

$$I_{\rm nth}(E_{21}, z_{\rm E}) = \frac{n^\infty_{\nu_1}(z_{\rm E})}{4\pi} = \frac{3}{11}\,\frac{\zeta(3)}{2\,\pi^3}\,T^3_{CMB}(z_E)\,, \tag{7}$$

where $n^\infty_{\nu_1}(z_{\rm E}) = (6/11)(\zeta(3)/\pi^2)\,T^3_{CMB}(z_E)$ is the relic neutrino number density at z_E in the standard stable neutrino case. This gives straightforwardly:

$$R \simeq R_\star \equiv \frac{6\,\zeta(3)}{11}\left[\frac{T_{CMB,0}\,(1+z_E)}{E_{21}}\right]^2 \simeq 3.5\times 10^5\,, \tag{8}$$

many orders of magnitude larger than R_E. However, this simplistic instantaneous description has the merit to show the natural normalisation for the specific intensity of the non-thermal photons in terms of $n^\infty_{\nu_1}(z_{\rm E})$ and for R itself in terms of $R_\star$.

Let us now calculate R removing the instantaneous assumption. Writing the fluid equation for the energy density of non-thermal photons produced by ν_1 decays [10,25,29],

$$\frac{d\varepsilon_{\gamma_{\rm nth}}}{dt} = \frac{\Delta m_1}{\tau_1}\,n^\infty_{\nu_1}(t)\,e^{-\frac{t}{\tau_1}} - 4\,\varepsilon_{\gamma_{\rm nth}}\,H\,, \tag{9}$$

where $H \equiv \dot a/a$ is the expansion rate, one easily finds a solution in terms of a Euler integral

$$\varepsilon_{\gamma_{\rm nth}}(t_E) = \frac{\Delta m_1}{\tau_1}\,n^\infty_{\nu_1}(t_E)\int_0^{t_E} dt\,e^{-\frac{t}{\tau_1}}\,\frac{a(t)}{a(t_E)}\,. \tag{10}$$

The integral is done over all times t when photons are produced by neutrino decays with energy Δm_1 that is redshifted to an energy $E(t, t_E) = \Delta m_1\,a(t)/a_E$ at t_E. Photons with the correct energy E_{21} at t_E are produced at a specific time t_{21} such that $a_{21}/a_E = E_{21}/\Delta m_1$, where $a_{21} \equiv a(t_{21})$. Of course notice that imposing $z_{\rm rec} > z_{21} \equiv a_{21}^{-1} - 1 > z_E$, one would find $E_{21} \lesssim \Delta m_1 \lesssim 0.35\,$meV, analogously to the range found for m_1 in the case $m_s \ll m_1$. However, since we are assuming that neutrinos are non-relativistic at decays, and this implies $T_\nu(z_{21}) \simeq 0.18\,$eV $(1 + z_{21})/(1 + z_{\rm dec}) \lesssim m_1 \lesssim 50\,$meV, one finds $z_{21} \lesssim 275$, implying an even more restrictive range

$$E_{21} \lesssim \Delta m_1 \lesssim 0.9\times 10^{-4}\,{\rm eV}\,. \tag{11}$$

We can now easily switch from time to energy derivative finding

$$I_{\rm nth}(E_{21}, z_E) = \frac{1}{4\pi}\,\frac{d\varepsilon_{\gamma_{\rm nth}}}{dE} = \frac{n^\infty_{\nu_1}(z_E)}{4\,\pi}\left(\frac{E_{21}}{\Delta m_1}\right)^{3/2}\frac{e^{-\frac{t_E}{\tau_1}\left(\frac{E_{21}}{\Delta m_1}\right)^{3/2}}}{H_E\,\tau_1}\,, \tag{12}$$

where $H_E \equiv H(t_E) \simeq 2/(3\,t_E)$. From the definition of R (see Eq. (6)) and $R_\star$ (see Eq. (8)), one immediately obtains

$$R = R_\star\left(\frac{E_{21}}{\Delta m_1}\right)^{3/2}\frac{e^{-\frac{t_E}{\tau_1}\left(\frac{E_{21}}{\Delta m_1}\right)^{3/2}}}{H_E\,\tau_1}\,. \tag{13}$$

The condition $R \le R_E$, where the equality corresponds to the condition to explain the EDGES anomaly and the inequality implies constraints on τ_1 and Δm_1, can be put in the simple form[12]

$$x\,e^{-x} = \frac{2}{3}\,\frac{R_E}{R_\star} = 2.2^{+4}_{-1}\times 10^{-6}\,, \tag{14}$$

where we defined

$$x \equiv \frac{t_E}{\tau_1}\left(\frac{E_{21}}{\Delta m_1}\right)^{3/2}\,. \tag{15}$$

There are clearly two solutions. A first one (referred to as 'EDGES A' in Fig. 2) for $\tau_1 \gg t_E$ is simply given by $x = 2.2^{+4}_{-1}\times 10^{-6}$, from which one finds

$$\tau_1 \ge 100^{+300}_{-65}\,t_0\left(\frac{10^{-4}\,{\rm eV}}{\Delta m_1}\right)^{3/2}\,, \tag{16}$$

where $t_0 = 13.8\,{\rm Gyr} = 4.35\times 10^{17}\,{\rm s}$ is the age of the universe. A second solution (referred to as 'EDGES B' in Fig. 2) is found for $\tau_1 \ll t_E$ and is given by $x = 15.2^{+1.8}_{-0.5}$, from which one finds

$$\tau_1 \le 2.10^{+0.04}_{-0.24}\times 10^5\,{\rm yr}\left(\frac{10^{-4}\,{\rm eV}}{\Delta m_1}\right)^{3/2}\,. \tag{17}$$

For this second solution one has to consider that decays should occur mainly after matter–radiation decoupling time in order to have a photon non-thermal background and one has to impose $\tau_1 \gtrsim t_{\rm dec} \simeq 3.71\times 10^5\,{\rm yr}$. Moreover, though photon energies are much below the thermal bath temperature, they might produce too large deviations of CMB from a thermal spectrum. Even though this second solution is less appealing and likely not viable, it is also interesting that one could in principle expect a number of neutrino species at recombination lower than three if only a fraction of the decays are allowed to occur before recombination.

[12] Of course one should also not forget that Δm_1 is constrained within the range in Eq. (11).

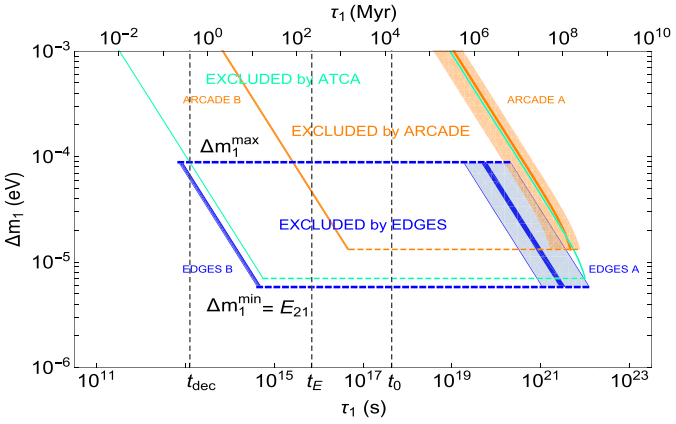

Fig. 2. The blue lines delimit the excluded region in the plane $\tau_1 - \Delta m$ from EDGES data and the two solutions (A and B) addressing the EDGES anomaly. The orange area indicates the approximate solution to the ARCADE 2 excess. The cyan area indicates the ATCA constraint. (For interpretation of the colours in the figure(s), the reader is referred to the web version of this article.)

We have now also to consider whether photons produced from neutrino decays might give visible (wanted or unwanted) effects at other frequencies. First of all one should worry of the CMB spectrum tested by the COBE-FIRAS instrument in the range of frequencies (2–21) cm^{-1} corresponding to (60–600) GHz or to energies (0.25–2.5) meV [30]. However, since $\Delta m_1 < 0.09$ meV (see Eq. (11)), in this non-relativistic scenario one completely circumvents the constraints from CMB thermal spectrum measurements.

Radio background observations in the GHz frequencies can also test the scenario either constraining it, as ATCA data do [23], or even providing, with the ARCADE 2 excess [22], another signal to be explained together with the EDGES anomaly.[13]

Let us see how they can be combined with 21 cm observations to test relic lightest neutrino decays. In this case the results are given in terms of an effective temperature $T_{\rm rb}(E_{\rm rb})$ of the radio background compared to the Rayleigh–Jeans tail of the CMB spectrum. This time the detection of the produced photons is made directly at the present time, while in the case of EDGES, as we discussed, photons produced by the decays are absorbed by the intergalactic medium at the time t_E. Therefore, now we have to impose

$$I_{\rm nth}(E_{\rm rb}, z=0) = \frac{n^{\infty}_{\nu_1}(z=0)}{4\pi}\,\frac{e^{-\frac{t(a_{\rm rb})}{\tau_1}}}{H(a_{\rm rb})\,\tau_1} = \frac{1}{4\pi^3}\,T_{\rm rb}\,E^2_{\rm rb}\,, \qquad (18)$$

where this time $a_{rb} = E_{\rm rb}/\Delta m_1$. If we focus on the solution at $\tau_1 \gg t_0$, then the exponential can be neglected and using $H(a_{rb}) = \sqrt{\Omega_{M0}\,a_{rb}^{-3} + \Omega_{\Lambda 0}}$ and defining $a^{M\Lambda}_{\rm eq} \equiv (\Omega_{M0}/\Omega_{\Lambda 0})^{1/3} \simeq 0.75$, one arrives to the condition

$$\tau_1 \geq \frac{6\,\zeta(3)}{11\,\sqrt{\Omega_{M0}}}\,\frac{T^3_{CMB,0}\left(\frac{E_{\rm rb}}{\Delta m_1}\right)^{3/2}}{T_{\rm rb}\,E^2_{\rm rb}}\left(1+\frac{a^3_{\rm rb}}{a^{M\Lambda}_{\rm eq}}\right)^{-1/2} t_0\,, \qquad (19)$$

where again the equality holds in the case one wants to explain the ARCADE 2 excess or the inequality in the case one imposes the constrain from the ATCA data. The ARCADE 2 collaboration claims an excess with $T_{\rm rb} = (62 \pm 10)$ mK at a frequency 3.2 GHz corresponding to $E_{\rm rb} = 13.2 \times 10^{-6}$ eV and from the condition (19) one finds

$$\tau_1 \simeq (800 \pm 200)\left(\frac{10^{-4}\,\text{eV}}{\Delta m_1}\right)^{3/2}\left(1+\frac{a^3_{\rm rb}}{a^{M\Lambda}_{\rm eq}}\right)^{-1/2} t_0\,, \qquad (20)$$

a solution shown in Fig. 2 ('ARCADE A') in orange (at 99% C.L.) together with the corresponding allowed range for Δm_1 found similarly to Eq. (11) with the difference that now the energy at the production has to be redshifted at $z = 0$ instead of $z = z_E$. If this is compared with the condition we found to explain the EDGES anomaly Eq. (16), one can see that within the errors the two anomalies can be reconciled, in particular for the lowest values of R_E corresponding to the highest τ_1 values, and of course with the help of a_{rb} as close as possible to unity (its maximum value), corresponding to $\Delta m_1 = E_{\rm rb}$. As in the case of the EDGES one can also consider a solution for $\tau_1 \ll t_0$ and in this case one finds, neglecting this time the small correction from Ω_Λ, $\tau_1 \simeq (70 \pm 0.7)$ Myr $(10^{-4}\,\text{eV}/\Delta m_1)^{3/2}$. This is also shown in Fig. 2 ('ARCADE B') in orange (at 99% C.L.). However, this time it is clear that there is no overlap with the 'EDGES B' solution and this somehow makes even more remarkable that in the case of $\tau_1 \gg t_0$ we could find two overlapping solutions. One can also consider the ATCA constraints [23] that place a $(3\,\sigma)$ upper bound $T_{\rm rb} \lesssim 100$ mK at a frequency of 1.75 GHz. In this case one finds the following (99%) excluded region

$$3.3 \times 10^5\,\text{yr}\left(\frac{10^{-4}\,\text{eV}}{\Delta m_1}\right)^{3/2} \lesssim \tau_1 \lesssim 660\left(\frac{10^{-4}\,\text{eV}}{\Delta m_1}\right)^{3/2}\left(1+\frac{a^3_{\rm rb}}{a^{M\Lambda}_{\rm eq}}\right)^{-1/2} t_0\,, \qquad (21)$$

shown in Fig. 2 in light green. Notice that this constraint does not apply to the narrow range $E_{21} < \Delta m_1 < E_{\rm rb} \simeq 7 \times 10^{-6}$ eV (so that EDGES allows to extend the constraints at slightly lower values of Δm_1).[14] Another interesting observation is that in the second stage of the evolution of T_{21} that we outlined in Section 2, for redshifts $250 \gtrsim z \gtrsim 30$, one expects an early absorption signal at $z \simeq 100$. If we extend the definition of R at a generic redshift $z_{\rm absorption}$, one can easily see from our expressions that this scales as $\propto \sqrt{1+z_{\rm absorption}}$. Therefore, the scenario predicts a doubled value of $R(z \simeq 100)$ compared to the one measured at z_E. This would be a powerful test of the scenario, though consider that in order to have a signal also in the early absorption stage, the upper bound on Δm_1 in Eq. (11) gets more stringent: from the requirement $z_{21} \lesssim 275$, now one obtains $\Delta m_1 \lesssim 3\,E_{21}$.

[13] Notice that in [31] the existence of the ARCADE 2 excess is questioned and it is proposed that a more realistic galactic model can reconcile measurements of uniform extragalactic brightness by ARCADE 2 with the expectations from known extragalactic radio source populations.

[14] Recently a study of the radio background data from the LWA1 Low Frequency Sky Survey (LLFSS) at frequencies between 40 MHz and 80 MHz [33] has found an excess well described by a power law $T_{\rm rb} \simeq T_{\rm rb,0}\,(\nu/\nu_0)^{\beta}$ with $\nu_0 = 310$ MHz and $\beta \simeq -2.58$, also fitting the ARCADE 2 results at much higher frequencies. For example at $\nu = 80$ MHz the survey finds $T_{\rm rb} = (1188 \pm 112)$ K. This excess cannot be explained by our model since from Eq. (19) one can see that it predicts $T_{\rm rb} \propto E^{-0.5}$. If we fit the ARCADE 2 results, then we have a signal at $\nu = 80$ MHz, approximately the same frequency tested by EDGES, that is about 100 times smaller than what LLFSS finds. Of course the LLFSS results do not exclude our model, they simply require an alternative explanation. More generally, they can be hardly reconciled with the EDGES anomaly within a realistic model since one would need a mechanism where the intensity of the produced radiation increases by about 20 times between $z \simeq z_E$ and today and this despite the fact that the expansion dilutes a matter fluid number density, such as primordial black holes, by a factor $(1+z_E)^3$. Even if one finds a model where this huge enhancement of the intensity is realised, this has to be strongly fine-tuned to match both results and this without considering the ARCADE 2 excess.

The derivation of the constraints could be further extended going beyond the quasi-degenerate limit $m_1 \simeq m_s$ implying necessarily going beyond the non-relativistic regime. In this case one has to take into account the thermal distribution function of neutrinos and from this derive the non-thermal distribution of photons solving a simple Boltzmann equation [32]. The factor R gets reduced for fixed τ_1 since the photon energy spectrum spreads at higher energies and at the energy E_{21} at z_E there are less photons and so the values of the lifetime that are necessary to explain the EDGES anomaly become shorter and this tends to generate a conflict with the constraints from radio observations and likely with the FIRAS-COBE data as well since photon energies can be much higher.

Finally, let us comment that though we have considered for definiteness decays of the lightest neutrinos, the results are also valid for heavier neutrinos of course with the replacement $(\tau_1, \Delta m_1) \rightarrow (\tau_{2,3}, \Delta m_{2,3})$. The only difference is that now they automatically respect the condition $m_{2,3} \gg 3\,\text{meV}$ to be non-relativistic and of course in this case the lower bound $m_1 \gtrsim 10\,\text{meV}$ does not hold so that the lightest neutrino mass can be arbitrarily small since lightest neutrinos do not play any role.

We should also say that of course, even though for definiteness we considered radiative decays into sterile neutrinos, our results are valid for any other decay mode involving a light exotic particle. Our results can also be easily exported to the case of quasi-degenerate dark matter recently proposed in [21] though notice that the correct way to calculate the specific intensity is Eq. (12) (replacing of course neutrino with dark matter number density) that takes into account that only those photons produced before t_E can be responsible for the signal while the authors of [21] incorrectly use an expression valid for photons detected at the present time. However notice that in the case of decaying dark matter the fact that the intensity of non-thermal photons has to be comparable to that of CMB photons, as required by EDGES, is a coincidence. On the other hand, in the case of decays of active to light sterile neutrinos, the abundance of relic active neutrinos is fixed by thermal equilibrium and this naturally produces a non-thermal photon intensity comparable to that of CMB photons. One can think of a simple model for example in terms of singular see-saw [34] extended with a type II contribution [35]. In this case an active–sterile neutrino mixing is expected and one can have interesting phenomenological consequences that can help testing the scenario.[15] For example, in addition to obvious possible effects in neutrino oscillation experiments and in particular in solar neutrinos, the fact that $m_s < m_1$ makes possible a mechanism of generation of a large lepton asymmetry in the early universe [36] with possible testable effects in big bang nucleosynthesis and CMB acoustic peaks [37].[16]

4. Conclusion

We discussed a scenario where relic neutrinos can radiatively decay into sterile neutrinos. This can be probed with 21 cm cosmology and, from EDGES results, we derived constraints on the mass and lifetime of the decaying active neutrino and on the difference of masses between active and sterile neutrino in the quasi-degenerate case. Interestingly, the scenario can explain the EDGES anomaly if this will be confirmed. The scenario could also potentially have other testable phenomenological effects such as the excess at higher radio frequencies claimed by the ARCADE 2 collaboration. Our results can be also straightforwardly extended to the case of decaying quasi-degenerate dark matter. Additional independent results on the global 21 cm signal from experiments such as SARAS [40] and LEDA [41] might provide independent tests of the EDGES anomaly. If this will be confirmed, a precise determination of the dependence of the absorption signal on redshift could potentially be used to test even more strongly our proposed scenario. Certainly 21 cm cosmology opens new fascinating opportunities to test models of new physics and might in a not too far future finally provide evidence of non-standard cosmological effects.

[15] Radiative decays would still generate an effective magnetic moment for active neutrinos but if the mixing the sterile neutrino is sufficiently small, a condition easily realised especially for the A solution with very long lifetime, this can be well below the upper bound from stellar cooling.

[16] One could investigate whether such dynamical generation of the asymmetry might suppress the thermalisation of a ∼eV sterile neutrino [38] required by the solution to the various anomalies [39].

Acknowledgements

PDB and MC acknowledge financial support from the STFC Consolidated Grant L000296/1. RS is supported by a Newton International Fellowship from Royal Society (UK) and SERB (India). KF acknowledges financial support from the NExT/SEPnet Institute. This project has received funding/support from the European Union Horizon 2020 research and innovation programme under the Marie Skłodowska-Curie grant agreement number 690575. We wish to thank Teppei Katori for useful comments.

References

[1] J.R. Pritchard, A. Loeb, Rep. Prog. Phys. 75 (2012) 086901, arXiv:1109.6012 [astro-ph.CO].

[2] S. Furlanetto, S.P. Oh, F. Briggs, Phys. Rep. 433 (2006) 181, arXiv:astro-ph/0608032.

[3] A. Cohen, A. Fialkov, R. Barkana, M. Lotem, Mon. Not. R. Astron. Soc. 472 (2) (2017) 1915, https://doi.org/10.1093/mnras/stx2065, arXiv:1609.02312 [astro-ph.CO].

[4] P.A. Oesch, et al., Astrophys. J. 819 (2016) 129, arXiv:1603.00461 [astro-ph.CO].

[5] J.D. Bowman, A.E.E. Rogers, R.A. Monsalve, T.J. Mozdzen, N. Mahesh, Nature 555 (7694) (2018) 67.

[6] R. Hills, G. Kulkarni, P.D. Meerburg, E. Puchwein, Concerns about modelling of foregrounds and the 21-cm signal in EDGES data, arXiv:1805.01421 [astro-ph.CO].

[7] R. Barkana, Possible interaction between baryons and dark-matter particles revealed by the first stars, Nature 555 (7694) (2018) 71, arXiv:1803.06698 [astro-ph.CO].

[8] D. Aristizabal Sierra, C.S. Fong, Phys. Lett. B 784 (2018) 130, https://doi.org/10.1016/j.physletb.2018.07.047, arXiv:1805.02685 [hep-ph].

[9] Z.G. Berezhiani, M.I. Vysotsky, V.P. Yurov, A.G. Doroshkevich, M.Y. Khlopov, Anomaly in Wien region of background radiation spectrum and radiative decay of relic neutral particles (In Russian), Sov. J. Nucl. Phys. 51 (1990) 1020, Yad. Fiz. 51 (1990) 1614.

[10] M.T. Ressell, M.S. Turner, The grand unified photon spectrum: a coherent view of the diffuse extragalactic background radiation, Comments Astrophys. 14 (1990) 323, Bull. Am. Astron. Soc. 22 (1990) 753.

[11] A. Mirizzi, D. Montanino, P.D. Serpico, Revisiting cosmological bounds on radiative neutrino lifetime, Phys. Rev. D 76 (2007) 053007, arXiv:0705.4667 [hep-ph];
J.L. Aalberts, et al., Precision constraints on radiative neutrino decay with CMB spectral distortion, arXiv:1803.00588 [astro-ph.CO].

[12] N. Aghanim, et al., Planck Collaboration, Astron. Astrophys. 596 (2016) A107, arXiv:1605.02985 [astro-ph.CO].

[13] K. Nakamura, S. Petcov, Particle Data Group, Neutrino masses, mixing and oscillations, Chin. Phys. C 40 (2016) 100001.

[14] M. Zaldarriaga, S.R. Furlanetto, L. Hernquist, 21 centimeter fluctuations from cosmic gas at high redshifts, Astrophys. J. 608 (2004) 622, arXiv:astro-ph/0311514.

[15] P.A.R. Ade, et al., Planck Collaboration, Planck 2015 results. XIII. Cosmological parameters, Astron. Astrophys. 594 (2016) A13, arXiv:1502.01589 [astro-ph.CO].

[16] P.C. Breysse, Y. Ali-Haïmoud, C.M. Hirata, arXiv:1804.10626 [astro-ph.CO].

[17] S.A. Wouthuysen, Astron. J. 57 (1952) 32;
G.B. Field, Proc. IRE 46 (1958) 240.

[18] A. Cohen, A. Fialkov, R. Barkana, M. Lotem, Mon. Not. R. Astron. Soc. 472 (2) (2017) 1915, arXiv:1609.02312 [astro-ph.CO].

[19] J.C. Hill, E.J. Baxter, Can early dark energy explain EDGES?, arXiv:1803.07555 [astro-ph.CO].

[20] N. Fornengo, R. Lineros, M. Regis, M. Taoso, Possibility of a dark matter interpretation for the excess in isotropic radio emission reported by ARCADE, Phys. Rev. Lett. 107 (2011) 271302, arXiv:1108.0569 [hep-ph];
L. Lopez-Honorez, O. Mena, A. Moline, S. Palomares-Ruiz, A.C. Vincent, The 21 cm signal and the interplay between dark matter annihilations and astrophysical processes, J. Cosmol. Astropart. Phys. 1608 (08) (2016) 004, arXiv:1603.06795 [astro-ph.CO].

[21] S. Fraser, et al., Phys. Lett. B 785 (2018) 159, arXiv:1803.03245 [hep-ph].

[22] D.J. Fixsen, et al., ARCADE 2 measurement of the extra-galactic sky temperature at 3–90 GHz, Astrophys. J. 734 (2011), 5, arXiv:0901.0555 [astro-ph.CO].

[23] T. Vernstrom, R.P. Norris, D. Scott, J.V. Wall, The deep diffuse extragalactic radio sky at 1.75 GHz, Mon. Not. R. Astron. Soc. 447 (2015) 2243, arXiv:1408.4160 [astro-ph.GA].

[24] M. Pospelov, J. Pradler, J.T. Ruderman, A. Urbano, New physics in the Rayleigh–Jeans tail of the CMB, arXiv:1803.07048 [hep-ph];
T. Moroi, K. Nakayama, Y. Tang, Axion–photon conversion and effects on 21 cm observation, arXiv:1804.10378 [hep-ph].

[25] E.W. Kolb, M.S. Turner, The Early Universe, Front. Phys., vol. 69, 1990.

[26] For an updated calculation of cosmological quantities such age of the universe and expansion rate, see for example, P. Di Bari, Cosmology and the Early Universe, CRC Press, ISBN 9781498761703, May 2018.

[27] C. Giunti, Nucl. Phys. B 908 (2016) 336, arXiv:1512.04758 [hep-ph].

[28] T. Sprenger, M. Archidiacono, T. Brinckmann, S. Clesse, J. Lesgourgues, arXiv:1801.08331 [astro-ph.CO].

[29] P. Di Bari, S.F. King, A. Merle, Dark Radiation or Warm Dark Matter from long lived particle decays in the light of Planck, Phys. Lett. B 724 (2013) 77, arXiv:1303.6267 [hep-ph].

[30] D.J. Fixsen, E.S. Cheng, J.M. Gales, J.C. Mather, R.A. Shafer, E.L. Wright, The Cosmic Microwave Background spectrum from the full COBE FIRAS data set, Astrophys. J. 473 (1996) 576, arXiv:astro-ph/9605054.

[31] R. Subrahmanyan, R. Cowsik, Astrophys. J. 776 (2013) 42, arXiv:1305.7060 [astro-ph.CO].

[32] E. Masso, R. Toldra, Phys. Rev. D 60 (1999) 083503.

[33] J. Dowell, G.B. Taylor, Astrophys. J. 858 (1) (2018) L9, arXiv:1804.08581 [astro-ph.CO].

[34] E.J. Chun, C.W. Kim, U.W. Lee, Phys. Rev. D 58 (1998) 093003.

[35] K.L. McDonald, B.H.J. McKellar, Int. J. Mod. Phys. A 22 (2007) 2211, arXiv:hep-ph/0401073.

[36] R. Foot, M.J. Thomson, R.R. Volkas, Large neutrino asymmetries from neutrino oscillations, Phys. Rev. D 53 (1996) R5349, arXiv:hep-ph/9509327;
P. Di Bari, R. Foot, Active sterile neutrino oscillations in the early universe: asymmetry generation at low $|\delta m^2|$ and the Landau–Zener approximation, Phys. Rev. D 65 (2002) 045003, arXiv:hep-ph/0103192.

[37] P. Di Bari, R. Foot, Active sterile neutrino oscillations and BBN + CMBR constraints, Phys. Rev. D 63 (2001) 043008, arXiv:hep-ph/0008258.

[38] R. Foot, R.R. Volkas, Phys. Rev. D 55 (1997) 5147, arXiv:hep-ph/9610229;
P. Di Bari, P. Lipari, M. Lusignoli, Int. J. Mod. Phys. A 15 (2000) 2289, arXiv:hep-ph/9907548.

[39] For a review see talk by M. Maltoni at Neutrino 2018, https://www.mpi-hd.mpg.de/nu2018/programme.

[40] S. Singh, et al., Astrophys. J. 845 (2) (2017) L12, arXiv:1703.06647 [astro-ph.CO].

[41] G. Bernardi, et al., Mon. Not. R. Astron. Soc. 461 (3) (2016) 2847, arXiv:1606.06006 [astro-ph.CO].